

Multi Focus Image Fusion with Region-Center Based Kernel

Ismail^{a,b,*}, Kamarul Hawari^a

^a Electrical and Electronics Engineering Department, Universiti Malaysia Pahang, Lebu Raya Tun Razak, Pahang, 26300, Malaysia

^b Electrical Department, Politeknik Negeri Padang, Limau Manis, Padang, 25126, Indonesia

Corresponding author: * ismail@pnp.ac.id

Abstract— The usage of the camera is ubiquitous nowadays. It provides highly accurate information. Then, the camera helps humans to carry out their specific tasks correctly. Furthermore, the camera becomes an important tool to achieve accurate computation in some fields, such as in medical diagnostic, robotics, remote sensing, and others. On the other side, the camera also has a weakness to capture detailed information of the scene in one image. Many images are needed to obtain the focus information of all the scenes since the lens's limitation depth of field produces out of focus regions beyond the focused object. To make a settlement of that case, the researchers have found a multi-focus image fusion process. This process selects all detailed information from a sequence of images and fuses them into one focused image. Through this fused image, the user such as human and machine can read the focus information easier. Later, the researchers developed multi-focus image fusion methods which various advanced procedures and algorithms. Furthermore, the implementation of multi-focus image fusion in new fields multiplied in the last two decades ago. It was able to create an accurate and efficient method to build a fused image. The proposed method is a kind of a new method in multi-focus image fusion. It works according to the region-center based kernel. The kernel processes input image to predict the detailed information of the scene. This method is robust to prevent the unexpected effects and sensitivities of noise. The proposed method generates a fused image with high accuracy. Finally, the assessment is done based on mutual information and structure similarity.

Keywords— Multi-focus image fusion; region-based kernel; high accuracy.

Manuscript received 20 Feb. 2020; revised 8 Nov. 2020; accepted 13 Dec. 2020. Date of publication 28 Feb. 2021.
IJASEIT is licensed under a Creative Commons Attribution-Share Alike 4.0 International License.



I. INTRODUCTION

The advancement of image processing applications can be found in many areas around us. There are many equipment types equipped with image processing principles available in the market, such as a handheld camera. They could be bought at a low price and can be easily found in the market with various types and models. It makes the camera become an essential device for acquiring data. They are practiced in

robotics, medical imaging, remote sensing fields, and others. There are some superiorities of a camera compare to other devices in the acquisition of accurate data. One of them is the camera's ability to catch detailed data or information objects more comfortably and efficiently. That is why the camera has become a ubiquitous device to help humans to do their works. Otherwise, the camera has a restriction on the depth of field (DOF). It makes the camera lens is not able to grab all detailed image scene in one capture portrait. A portrait contains only one region of focus view (see Fig. 1).

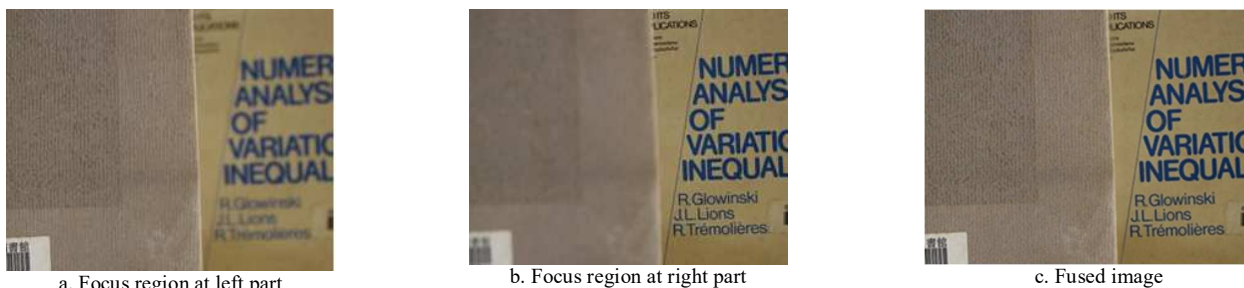


Fig. 1 Two images with different focus region (a,b) and fused image (c)

Also, the collection of all focus views in one image are obtained through gathering focus regions from a sequence of images. The process of generating all in a focused image from a partially focused image is term as image fusion [1]. The development of multi-focus image fusion has taken place by researchers for many years. The new and advanced techniques have been found and spread so far. These efforts were applied in many fields. Further, there was a various method exists in multi-focus image fusion. They were commonly divided into two methods: the spatial and the transform domain method [2].

Firstly, the spatial domain method is the method that fuses multi-focus images directly into the fused image. This method can be found in the form of the region or block-based method. The region based on image fusion is put in feature-based image fusion in some scientific articles [3]. This category is supported by using probability filtering and the region correction method to generate a fused image [4]. In order to sharpen the focus region and decrease computation cost, the applying Laplacian kernel is implemented in [5]. Then, the optimization method of kernel processing and subsampling sample is applied in [6]. The other method predicts the focus region through the mean shift algorithm to create the precise segmentation map [7]. Then, by using the image's information saliency, the method is supposed to keep the detailed information of multi-focus images in constructing the fused image [8].

Furthermore, in achieving a better output, the fused image is generated from the content-based blurring region with an adaptive threshold [9]. The other method computes intersection points to find focus boundaries[10]. The cartooned focus object is used in [11]. The use of various imaging plane positions can obtain data from the focus region as in [12]. On the other side, the transform domain method is where the input image transformed into a frequency domain to fuse two or more input images and finally inverse it back to the spatial domain. The transform domain's use with the selected coefficient is then fused to create a fused image[13]. Then, wavelet transform is used to determine high and low frequencies; these two poles are then trained with Deep CNN [14].

Furthermore, wavelet transform is used to detect fusion weight and then optimized with Guided Image Filter[15]. The other method uses wavelet transform in $YCbCr$ color space[16]. Finally, wavelet transform is used to decompose focus images into high and low frequencies, then a deep CNN is applied to make the model of mapping[17] and so on.

II. MATERIAL AND METHOD

There are some designs of filters available in image processing nowadays. Each of them has a special characteristic to obtain the needed information from the input. The double band filter successes in detecting the signal in the network[18]. Sampling kernel-based filter increases efficiency more than using an algorithm filter[19]. The circular shape filter can give very low distortion to the image[20]. The above filters apply pixel-based in the center of the kernel. A pixel in the center kernel will be the output value of the convolution.

The proposed method does not use pixel-based in the center of the kernel. Otherwise, the center of the kernel is operated

by a region whose size varies depending on the case. It is called a region-center based kernel.

The design of the sliding window is generally seen in Figure 1. The kernel size is N . The center pixels is M . The center pixels represent the sliding window's neighborhood values. The neighborhoods have a great influence on deciding. Sometimes, this value's accuracy shows the uncertainties and tends to produce unexpected effects and high sensitivity. Many kinds of kernel properties are available that determine the filter attributes, which influence the output image[21]. So, the filter has a specific purpose depending on the kernel properties. Generally, the filter makes smoothing images, removing the noise, finding the feature of the image, and so on.

The performance of the kernel is determined by the kernel size and weigh filter too. The bigger the kernel size, the more accurate the kernel is. Then the values of the center pixel automatically to be the filtering output. The sliding window operates from left to right and from top to bottom. To convolve the whole regions of the image, the image padding is added to the input image. In the end, the image padding is removed.

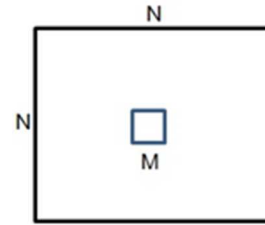


Fig. 2 The general design of filter kernel

The Fig. 2 above shows a kernel with a pixel in the center. Where, N is the kernel size, usually an odd number. M is the center pixel. The size of M is usually one (1) pixel. This center pixel value is the result of the multiplication or convolution process from the neighborhood. Sometimes, the center-pixel kernel can produce output with unwanted effects that can degrade the contrast of the image. The author proposes a new method to solve these difficulties, and a new kernel design supports the new method. The proposed kernel architecture is composed of the wide center region. This kernel is termed as region-center based kernel. The design is as Fig. 3 below.

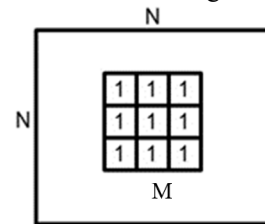


Fig. 3 The design of region-center based kernel

Fig. 3 shows a region-center-based kernel with the center-kernel size $M \times M$. The $N \times N$ is the size of the sliding window, and M is the size of row and column of the region-center kernel. An all-one matrix occupies the region-center space with size three by three, J_m . Where, $J_m = e m e^T = 1$ [21]. Where e_m is the vector one. The region-center based kernel purposes are to handle sensitivity and the unpredicted problem of the pixel-based kernel operation. Furthermore, the proposed method gives more presence of texture and other pixel profiles. It is a feature of the focus region.

A. Image Gradient

Image gradient is a directional alteration of image intensity or image color. This alteration has a magnitude and direction. In the image processing, a gradient image is presented in 2D space. Mathematically, the gradient image is derived from the vertical and horizontal directions. At each pixel, the gradient vector points out in the direction of the largest possible intensity increase, and the length of the gradient vector corresponds to the rate of change in that direction. Image gradient is the vector of its partial derivatives that can also measure image quality[22]. Mathematically, it is formulated as follow:

$$\nabla I = \begin{pmatrix} g_x \\ g_y \end{pmatrix} = \begin{pmatrix} \frac{dI}{dx} \\ \frac{dI}{dy} \end{pmatrix} \quad (1)$$

Based on Equation 1, dI/dx is the derivative respected to the x -axis, and dI/dy is the derivative respected to the y -axis.

B. Morphological Filter

The morphological filter operation is a non-linear operation related to a feature image's appearance or morphology [23]. Here, it is used to round up the numerous imperfections of shape from the initial focus region. The morphological filter can improve the structure of the binary or grayscale image. This operation explores the image using a structuring element. The structuring element is a small shape that places on all possible regions of the image. The response is obtained by comparing it with the neighborhood. The operation of the structure element is like a convolution kernel operation in linear image filtering. There are some common operations of morphological filtering[23].

1) *Erosion Operation*: The erosion operation is a combination of two sets using the set elements' vector intersection. Mathematically, the erosion of set A by set B is formulated as follow:

$$E(R, S) = R \ominus \check{S} \quad (2)$$

Where

$$R \ominus \check{S} = \overline{\overline{R} + S} \quad (3)$$

\overline{R} is a complement of R.

2) *Dilation Operation*: The dilation operation is a combination of two sets using vector summation of the set elements. The dilation of set R by set S is mathematically formulated as follow:

$$D(R, S) = R \oplus \check{S} \quad (4)$$

Where \square is the vector supplement and \check{S} reflects S through the origin of S. The wide application of erosion and dilation are closing and opening operation. The closing and opening operations work fundamentally supported by erosion and dilation. The operations give a specific characteristic to the filtered image. The detail of the closing and opening operation is as follow:

3) *Closing Operation*: The closing operation is the unification of both erosion and dilation operations. It is a sequence of procedures. The procedure is started with erosion and is followed by a dilation operation. If the set of R

performs a closing operation to a set of S, then the mathematical equation as follows:

$$C(R, S) = D(E(R, S), \check{S}) \quad (5)$$

Where C symbolized the closing operation.

4) *Opening Operation*: The opening operation is also a sequence of morphological operations consists of dual procedures, dilation, and erosion operations. It performs dilation and erosion operations consecutively. The mathematical equation of the opening operation is as the following equation.

$$O(R, S) = E(D(R, S), \check{S}) \quad (6)$$

The opening operation is symbolized with O.

The multi-focus image fusion with region-center based kernel is a kind of a new method. The process emphasizes generating stability of the initial focus region. The region-center-based kernel mainly supports the stability of the initial focus region. Region-center based kernel is a kernel or sliding window representing the neighborhood values through a region or unification of some pixels. The region describes the neighborhood profile of input images. The decision of the sliding window offers the label to estimate the focus region.

The process of labeling is performed by comparing the gradient magnitude between two input images. The gradient magnitude of both kernels from two input images are compared. If the first kernel operates on the gradient of image 1 and another operates on the gradient of image 2. The profile gradient maps from two kernels are accumulated. The kernel, which has a higher magnitude gradient, is labeled to interpret for an initial focus map. If the gradient from the block region of input image 1 is higher, then the all-one matrix gives a label to initial focus region map 1, and vice versa. The all-one matrix is sized in three by three. This process delivers an initial focus region, IFR. The IFR procedure is based on Equation 7 and Equation 8 below:

$$IFR_1(x, y) = \begin{cases} J_{m1} = 1, & \nabla_1(x, y) \geq \nabla_2(x, y) \\ J_{m1} = 0, & \text{Otherwise} \end{cases} \quad (7)$$

$$IFR_2(x, y) = \begin{cases} J_{m2} = 1, & \nabla_1(x, y) < \nabla_2(x, y) \\ J_{m2} = 0, & \text{Otherwise} \end{cases} \quad (8)$$

Equation 7 and Equation 8 above show the parameters of forming the initial focus region. Where, $J_{m1} = 1$ is the central region of the kernel with the all-one matrix, the size is three by three (3x3). The region-center-based kernel is a projection of the center pixel kernel with a certain scale. The description of region-center-based kernel and the process of labeling initial focus map are shown in Fig. 4.

In the block diagram below shows the generating of the initial focus map. It is generated through a region-center based kernel. The sliding window reads the neighborhood's information, and the result is a spatial region or all-one matrix with a size 3 x 3. It is very different from the common sliding windows that produce a pixel value only as a center pixel. Also, through the region-center based kernel, it can handle noise sensitivity and unstable pixel. This process is fundamental in this algorithm since the work is very simple, fast and accurate. The obtained focus map shows high

stability and accuracy. The following process of the algorithm will take place with a very simple and at low cost.

The filter compares both input images through the sliding window's pixel intensity, then computes and compares the pixel intensity to all input images' surfaces. This comparison will generate the predicted focus gradient. This map becomes the important data to be processed in order to find the focus region.

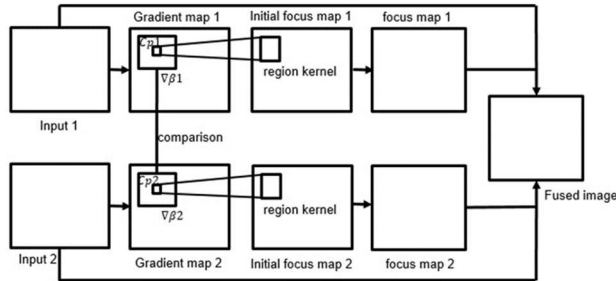


Fig. 4 The block diagram of the proposed method

The region-center based kernel works with more powerful. Since it is a regional scale, it works higher cost than pixel kernel. However, the higher cost of processing does not have much influence on time-consuming on a computer. Generally, nowadays computers run in high technical specifications.

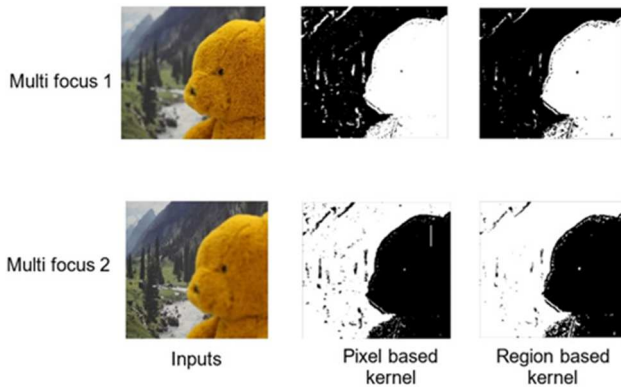


Fig. 5 Initial focus region map from multi-focus images

Fig. 5 shows the comparison of the initial focus region according to pixel-center based kernel and region-center based kernel. The input images are the bear toy with a diverse of textures at the background. The focus and out-of-focus regions are almost similar. The pixel-center based kernel remains them with the noise. Nevertheless, the region-center-based kernel can make the background noise into tiny objects. The tiny objects are more comfortable to remove or collect in the next step.

The condition with focus and out-of-focus regions looks similar also appears in Fig. 6. The input images have a background with the black color region. These black regions look the same in focus and out-of-focus conditions. The pixel-based kernel is challenging to recognize black regions in focus and out-of-focus conditions. It leaves a quite large shape of the unexpected region. Otherwise, the region-center-based kernel can handle that problem. The focus and out-of-focus region have separated with different properties.

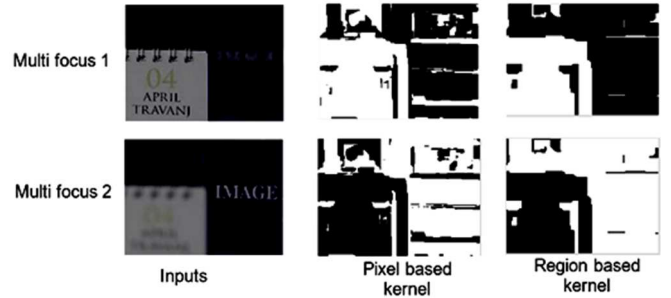


Fig. 6 Initial focus region map from multi-focus images

The following stage determines the focus region after the initial focus regions were built. The focus region's generating is created through the morphological filter, which converts the initial focus-region map to become a focus region map, FR. The operation involves a morphological filter, as shown in Equations 9 and 10.

$$FR^{M,N} = RNO((IFM^{M,N}), K) \quad (9)$$

The RNO is a morphological operation that purposes to remove noise or small objects (RNO). $FR^{M,N}$ is a focus region map of both M and N images. K is the block size. The morphological filter works based on window kernel operation. The kernel selects the object that has the attribute to be removed.

Second, we perform integrating disconnecting parts of the region (IDR) operation. The sliding window is also applied to this operation. The purpose of this operation is to collect and combine as much as possible related objects. Further, this operation also improves the less perfected connection. It raises the genuine character of the object's shape. The other aim of the operation is to cover the holes or small black points on the object. The operation has the equation as follow:

$$FR^{M,N} = IDR((IFR^{M,N}), K) \quad (10)$$

Those above stages of processes can manage the transformation of the initial focus map into a focus map. The focus map completion is shown in Fig. 7.

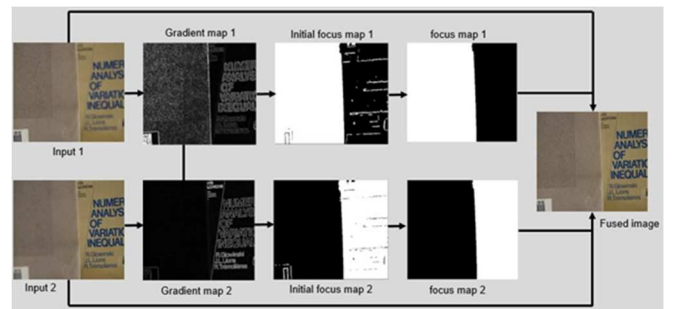


Fig. 7 The complete of block diagram of the proposed method

The last equation (Equation 11) creates a fused image (I^{fused}) based on a fusion focus map and multi-focus images. The whole processing is as shown in Figure 7. The input images that have perfect information about the objects remain. Through a simple and easy procedure, we can generate a fused image with high accuracy. The detailed result is shown in Figure 8.

$$I^{fused} = FR^M * I^M + FR^N * I^N \quad (11)$$

III. RESULTS AND DISCUSSION

The results of the proposed algorithm have a high accuracy of the fused image. The parameter to measure the accuracy is as other researchers used. The result quality assessment is based on mutual information [24] and structure similarity [25]. The mutual information measures the completeness of information come from the input images and fused image. This method assesses the number of information lost because of algorithm processing. The comparison between similar information of fused image and input images is shown in the following equation:

$$MI_{fused}^{M,N} = \left[\frac{I(fused,M)}{H(fused)+H(M)} + \frac{I(fused,N)}{H(fused)+H(N)} \right] \quad (12)$$

MI is the mutual information between the fused image (fused) and input images (M, N). $I(fused, M)$ is the mutual information between fused image and input image M, and $I(fused, N)$ is mutual information fused image and the input image, N. $H(fused)$, $H(M)$, and $H(N)$ are entropy of fused image, an input image, M and input image, N respectively [24].

Otherwise, the measure of structure similarity is a measurement of detailed information between fused images and input images. The fused image and input image's focus region is assessed to obtain the structural similarity among them [25]. The measurement is based on the equation below:

$$SSIM(M, fused) = \frac{(2\mu_M\mu_N+C_1)(2\sigma_{MN}+C_2)}{(\mu_M^2+\mu_N^2+C_1)(\sigma_M^2+\sigma_N^2+C_2)} \quad (13)$$

The $C1 = (K1L)^2$; $C2 = (K2L)^2$, L is dynamic range (255), $K1 = 0.01$ and $K2 = 0.03$. The SSIM is structure similarity between reference image (M) and fused image (fused). The maximum value is 1. It means the two images are identical properties. The μ is mean intensity, and σ is variance intensity. Based on the SSIM and MI method, we measure the fusion quality objectively. The assessment of image fusion examines the degradation of structural information. We obtain that our method does not lose significant structural data.

A. Experiment and Result

The experiments of proposed methods are done by applying some different multi-focus images as a dataset. The images are created by using a general handheld camera available in the market. The arrangement of focus lens distance determines the focus parts of the input image. This process is available in the rotary adjustment focus lens on the camera device. The placement of proper focus zone camera to the object produces the object in the focus region, but the background is in the out of focus region of the image. Otherwise, a set of focus lens on the background produces the out of focus region on the object.

Commonly two input images are needed in multi-focus image fusion processing, include in this algorithm. Both images are then treated as source information.

The proposed method operates with different sources of image properties. The first one is a pair of the greyscale image from the common dataset. They are generally applied in almost multi-focus image fusion papers. It is as shown in figure 9 (the lab).

Secondly, the method also implemented with input color images. The author creates some pairs of multi-focus images. There are five pairs of different multi-focus images. These input images are as shown in Fig. 8. All images have applied to the proposed algorithm. The pair of images are placed in the first and second column from the left side on Fig. 8. The output image or fused image are placed at the rightest column in Fig. 8.

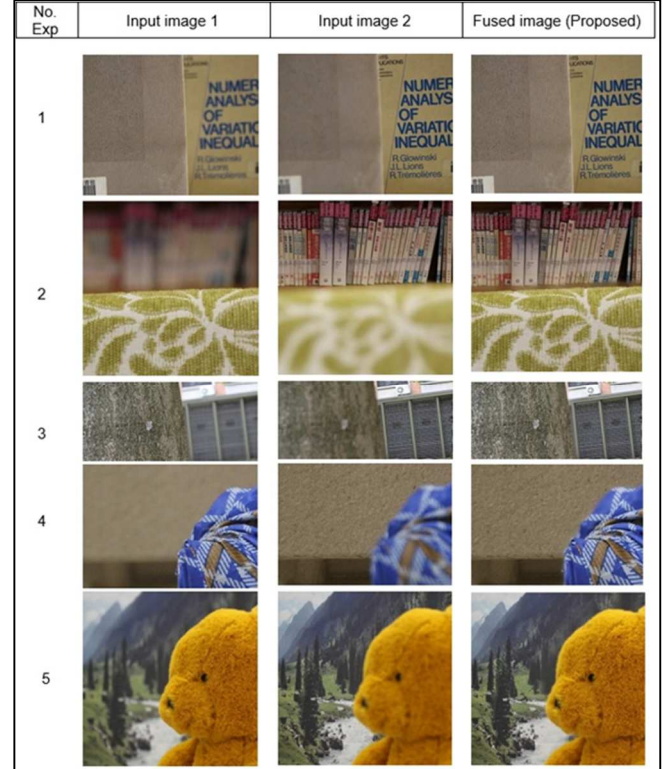


Fig. 8 The results of the proposed method with different images

In Fig. 8, the first row is experiment number 1. The two input images are a figure of the book. The first input, the focus regions on the left side, the right is blurred. On the second, the blurred region is on the left and focus region is on the right part. Finally, the fused image or output is in the rightest column. The result is apparent and stable. It means that both input images could have a perfect synthesis. The border between focus and blurred region diminished. It left just one region, all in the focused image.

The assessment is done according to the mutual information and structural similarity methods to measure the fused image's quality. These assessments perform the fused image of experiment number 1. The obtained quality indexes are presented in Table 1 on the first row (top row). The MI index is 0.7719. It means that the fused image's collected information has a little bit of loss in the processing stages. The structural similarity (SSIM) index for experiment 1 is 0.8584. In general, the structure of the input image and output image almost the same. The same process also implemented to other four pair input images—experiment number 2 up to number 5.

It is a bit different between the experiment number 5 with other experiments number 1 – 4. In experiment number 5, the input data has a dynamic scene. It means the method also implemented in the condition where the object or background

has a moving. The obtained indexes of the scene are 0.7605 and 0.7269 for MI and SSIM, respectively.

As the proposed method purpose can serve important information from input images into a single image with high accuracy and low cost, the assessment quality shows the output images are acceptable. Through subjective opinion, in the output images are contained all the focus information.

The process succeeded in generating focus regions for every input image. It runs successfully to lay down focus regions on fused image. The appearance of region boundaries in the fused image does not significantly affect the whole region of the fused image. There are some glowing or luminous regions in experiment number 4, caused by some unpredicted light. Nevertheless, the proposed method is still able to handle it.

Our proposed method is also compared with other multi-focus image fusion methods such as Dense SIFT [26], and gradient-domain [27]. The comparison is in grayscale and color images. For the grayscale image, the picture is the lab. The output image is as shown in figure 9. The metric indexes are shown in Table 1 (third row). Then, the color image as the input image is also implemented in the comparison—the result is shown in Fig. 10 (left column). The assessment quality indexes are shown in Table 2.

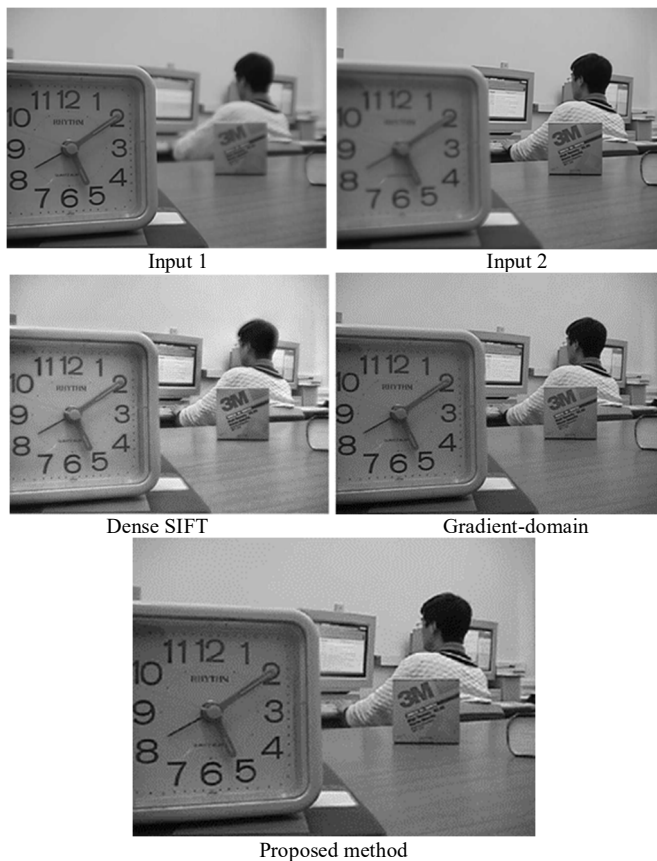


Fig. 9 The comparison our method with some others for grey image

In the experiment with greyscale images, the mutual information index is 0.7521, and the SSIM index is 0.9220. The comparison with Dense SIFT and MW gradient method in detail, as shown in Table 1. The experiments were also performed on color images. The fused images are also measured based on Mutual Information (MI) and Structure Similarity (SSIM). The result of applying color images as

source input is as presented in Fig. 9. The objective measurement of our method assesses the proposed algorithm is presented in Table 2.

TABLE I
METRIC INDEXES

No Experiment	Mutual Information Index	SSIM Index
Dense SIFT	0.7479	0.8795
Gradient	0.6735	0.7761
Proposed	0.7521	0.9220

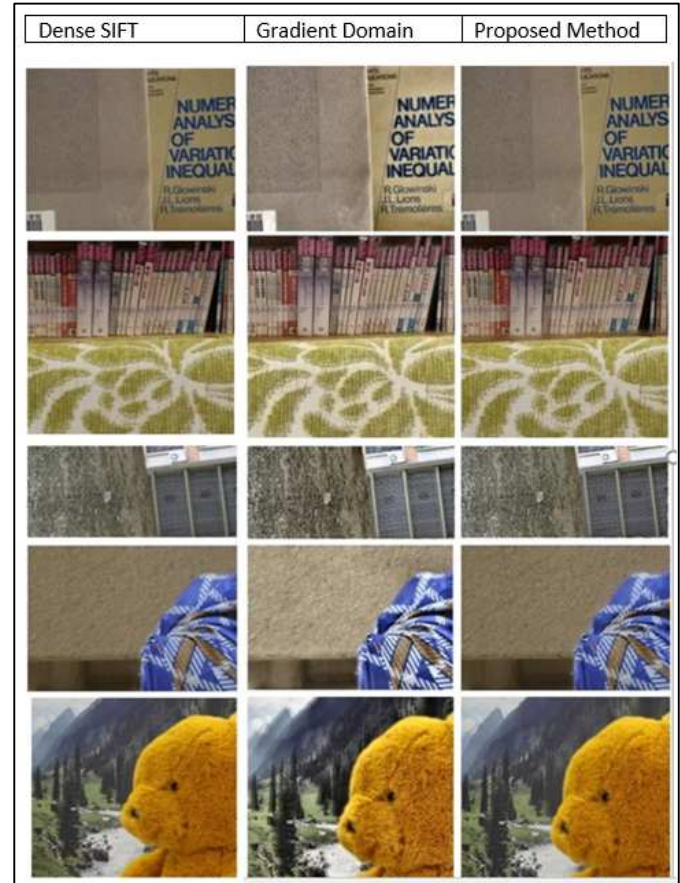


Fig. 10 The Fusion result of some color images (experiment 1-5), the column title points out the method used to obtain fused image

TABLE II
ASSESSMENT QUALITY INDEXES

No. Exp	Dense SIFT		MW Gradient		Proposed	
	MI Index	SSIM Index	MI Index	SSIM Index	MI Index	SSIM Index
1	0.7719	0.8554	0.3790	0.4021	0.7724	0.9268
2	0.8502	0.6037	0.4521	0.3182	0.8490	0.6567
3	0.7716	0.7211	0.3172	0.5603	0.7719	0.7723
4	0.7654	0.6588	0.4667	0.3873	0.7596	0.7947
5	0.7605	0.7269	0.4369	0.4388	0.7546	0.7664

Fig. 10 shows the fused images taken from color input images. Based on the human eye, for experiment number 1, the gradient domain method shows more brightness than the other two methods. This situation also exists in experiment number 2 to 5; the proposed method and Dense SIFT method show almost similar brightness for all experiments.

Based on objective measurement, the Mutual Information index, and Structural Similarity (SSIM) are shown in Table 2.

The proposed method shows a better result on the SSIM index than the other two methods. The algorithm has robust spatial domain processing so that it has a strong structure on the fused image. The Mutual Information index of the proposed method is vital on experiment number 1 and number 3. The Dense SIFT has a little lost information during the data processing stage.

Although our method does not gain the top Mutual Information index for all experiments, it does not mean that our method loses much information during the fusion process. The Mutual Information index is still in the acceptable range when compared with other methods. Finally, the multi-focus image fusion with region-center-based kernel has the strong ability to keep the detail of the input images in the fused image.

IV. CONCLUSION

This paper presents a novel method in multi-focus image fusion. The method is succeeded to applied the region-center-based kernel to determine the initial focus region map. Using a region-center-based kernel on a sliding window helps minimize pixel sensitivity and unexpected result. These evaluation results describe that the proposed method has the robustness to keep the detail or essential information of the input images. This method is low cost, so it is easy to be implemented in many relevant fields such as robotics and medical diagnostics.

ACKNOWLEDGMENT

The Kemdikbud scholarship supports this article.

REFERENCES

- [1] Y.Liu, L.Wang, J.Cheng, C.Li, and X.Chen, "Multi-focus image fusion: A Survey of the state of the art," *Inf. Fusion*, vol. 64, no. April, pp. 71–91, 2020.
- [2] S.Masood, M.Sharif, M.Yasmin, M. A.Shahid, and A.Rehman, "Image fusion methods: A survey," *J. Eng. Sci. Technol. Rev.*, vol. 10, no. 6, pp. 186–194, 2017.
- [3] B.Meher, S.Agrawal, R.Panda, and A.Abraham, "A survey on region based image fusion methods," *Inf. Fusion*, vol. 48, no. December 2017, pp. 119–132, 2019.
- [4] X.Xia, Y.Yao, L.Yin, S.Wu, H.Li, and Z.Yang, "Multi-focus image fusion based on probability filtering and region correction," *Signal Processing*, 2018.
- [5] A. G.Felix and C.Juan, "Multi-focus image fusion for multiple images using adaptable size windows and parallel programming," *Signal, Image Video Process.*, no. 1, 2020.
- [6] A.Garnica-Carrillo, F.Calderon, and J.Flores, "Multi-focus image fusion by local optimization over sliding windows," *Signal, Image Video Process.*, vol. 12, no. 5, pp. 869–876, 2018.
- [7] S.Tello-Mijares and J.Bescós, "Region-based multifocus image fusion for the precise acquisition of Pap smear images," *J. Biomed. Opt.*, vol. 23, no. 05, p. 1, 2018.
- [8] D. P.Bavirisetti and R.Dhuli, "Multi-focus image fusion using multi-scale image decomposition and saliency detection," *Ain Shams Eng. J.*, vol. 9, no. 4, pp. 1103–1117, 2018.
- [9] M. S.Farid, A.Mahmood, and S. A.AI-Maadeed, "Multi-focus image fusion using Content Adaptive Blurring," *Inf. Fusion*, vol. 45, no. January 2018, pp. 96–112, 2019.
- [10] M.Nejati *et al.*, "Surface area-based focus criterion for multi-focus image fusion," *Inf. Fusion*, vol. 36, pp. 284–295, 2017.
- [11] Z.Liu, Y.Chai, H.Yin, J.Zhou, and Z.Zhu, "A novel multi-focus image fusion approach based on image decomposition," *Inf. Fusion*, vol. 35, pp. 102–116, 2017.
- [12] C.Ho, "Multi-Focus Image Fusion and Depth Map Estimation Based on Iterative Region Splitting Techniques," *MDPI*, 2019.
- [13] G.Pajares and J. M.dela Cruz, "A wavelet-based image fusion tutorial," *Pattern Recognit.*, vol. 37, no. 9, pp. 1855–1872, 2004.
- [14] J.Li, G.Yuan, and H.Fan, "Multifocus image fusion using wavelet-domain-based deep cnn," *Comput. Intell. Neurosci.*, vol. 2019, 2019.
- [15] M. M. I.Ch, M. M.Riaz, N.Iltaf, A.Ghafoor, and S. S.Ali, "A multifocus image fusion using highlevel DWT components and guided filter," *Multimed. Tools Appl.*, vol. 79, no. 19–20, pp. 12817–12828, 2020.
- [16] T.Ransform, P. C. A.On, and Y. C.Olor, "Multi-Focus Image Fusion Based on Stationary Wavelet," *J. Southwest Jiaotong Univ.*, vol. 54, no. 5, 2019.
- [17] J.Li, G.Yuan, and H.Fan, "Multifocus image fusion using wavelet-domain-based deep cnn," *Comput. Intell. Neurosci.*, vol. 2019, 2019.
- [18] J.Dash, B.Dam, and R.Swain, "Design of multipurpose digital FIR double-band filter using hybrid firefly differential evolution algorithm," *Appl. Soft Comput. J.*, vol. 59, pp. 529–545, 2017.
- [19] K. J.Kim, J. H.Kim, and S. W.Nam, "Design of computationally efficient 2D FIR filters using sampling-kernel-based interpolation and frequency transformation," *Electron. Lett.*, vol. 51, no. 17, pp. 1326–1328, 2015.
- [20] R.Matei and D.Matei, "Circular IIR Filter Design and Applications in Biomedical Image Analysis," *Proc. 10th Int. Conf. Electron. Comput. Artif. Intell. ECAI 2018*, pp. 1–6, 2019.
- [21] W. R. E.Gonzalez R C, *Digital Image Processing, Third Edition, An adopted version*. Pearson, 2008.
- [22] W.Lyu, W.Lu, and M.Ma, "No-reference quality metric for contrast-distorted image based on gradient domain and HSV space," *J. Vis. Commun. Image Represent.*, vol. 69, p. 102797, 2020.
- [23] Y.Zhang, X.Bai, and T.Wang, "Boundary finding based multi-focus image fusion through multi-scale morphological focus-measure," *Inf. Fusion*, vol. 35, pp. 81–101, 2017.
- [24] B.Xiao and L.Yan, "An objective image fusion performance index: Normalized edge mutual information," *Proc. 30th Chinese Control Conf. CCC 2011*, vol. 2, no. 1, pp. 3025–3028, 2011.
- [25] Z.Wang, A. C.Bovik, H. R.Sheikh, and E. P.Simoncelli, "Image quality assessment: From error visibility to structural similarity," *IEEE Trans. Image Process.*, vol. 13, no. 4, pp. 600–612, 2004.
- [26] Y.Liu, S.Liu, and Z.Wang, "Multi-focus image fusion with dense SIFT," *Inf. Fusion*, vol. 23, pp. 139–155, 2015.
- [27] S.Paul, I. S.Sevcenco, and P.Agathoklis, "Multi-exposure and multi-focus image fusion in gradient domain," *J. Circuits, Syst. Comput.*, vol. 25, no. 10, pp. 1–18, 2016.